T-AES/25/4//28649

Analytic Example of a Schweppe Likelihood-Ratio Detector

Thomas H. Kerr

Reprinted from
IEEE TRANSACTIONS ON AEROSPACE AND ELECTRONIC SYSTEMS
Vol. 25, No. 4, July 1989

Analytic Example of a Schweppe Likelihood-Ratio Detector

THOMAS H. KERR, Senior Member, IEEE
M.I.T. Lincoln Laboratory

As investigators seek to verify various computer implementations of Schweppe's likelihood detector in a variety of different applications from radar and sonar to general statistical hypothesis testing on received signals, it is useful first to validate software performance by using a low-dimensional test problem of known solution, as offered here. A closed-form solution is provided here for a Schweppe likelihood detector in terms of an intermediate Kalman filter, as utilized in its implementation, for detecting the presence of a two-state signal model in Gaussian white noise. The associated error probabilities are also evaluated following a procedure, developed by Van Trees, which utilizes optimized Chernoff-like bounds for a tight approximation. A methodology is demonstrated for appropriately setting the decision threshold for this example as a tradeoff against allowable observation time. By using this or similar examples, certain qualitative and quantitative aspects of the software implementation can be checked for conformance to anticipated behavior as an intermediate benchmark, prior to modular replacement of the various higher-order matrices appropriate to the particular application. This procedure is less expensive in central processing unit (CPU) time during the software debug and checkout phase than using the generally higher n-dimensional matrices of the intended application since the computational burden is generally at least a cubic polynomial in n during the required solution of a matrix Riccati equation.

Manuscript received February 3, 1989.

IEEE Log No. 28649.

This work was supported by the United States Department of the Air Force under Contract F19628-85-C-0002.

Author's address: M.I.T. Lincoln Laboratory, 244 Wood St., P.O. Box 73, Lexington, MA 02173.

I. INTRODUCTION

Low-dimensional 1-, 2-, and 3-state test cases such as those of [1, pp. 125–127, pp. 138–142, pp. 243–244, p. 246, pp. 255–257, pp. 319–320], [2, p. 184, pp. 186–188], [3–12], [13, pp. 256–257, pp. 281–282], [23], [25] have been extensively used to verify software performance of newly coded implementations for Kalman filter applications. The benefits of doing so are the reduced computational expense incurred during software debug by using these low-dimensional test cases and the insight gained into software performance as gauged against test problems of known solution. A modular software design must be adopted in order to accommodate this approach, so that upon completion of successful verification of the objective computer program implementation with these low-dimensional test problems, the matrices corresponding to the actual application can be conveniently inserted as replacements without perturbing the basic software structure and interactions between subroutines. (Only certain time-critical, real-time applications would defy handling in this manner by needing matrix dimensions that are "hardwired" to the particular application.) This paper similarly offers a simple transparent and tractable two-dimensional example that can be used to verify any software implementation of the Schweppe likelihood-detector. Simultaneously, this presentation constitutes a quick overview of all the relevant aspects of a Schweppe likelihood detector implementation along with conditions of applicability that must be checked as a rationale for the correctness of what is being presented. Without this accompanying substantiation, it would be pointless to check software performance against a target solution unless veracity of this test case were assured. By establishing the pedigree of the solution advertised here, subsequent software verifiers, when faced with verifying and validating newly coded Schweppe likelihood subroutine software modules, can treat the entire exercise as one of confirming the proper performance behavior of the new module as a black box by just confirming the outputs without having to understand the internal intricacies. Thus their job is simplified by the results presented here.

The landmark Schweppe likelihood detector [15] is discussed extensively in both [17] and in [14], and a methodology was first presented in [18] for evaluating the associated receiver operating characteristics (ROC) consisting of the probabilities of false alarm and miss, also known as one minus the probability of correct detection. In the parlance of statistical hypothesis testing, these are the probabilities of error of the first and second kind, respectively. Correctly implementing a Schweppe likelihood ratio is, in general, more challenging than simply implementing a Kalman filter with its associated Riccati equation for the time evolution of the covariance of the

estimation error. In fact, the Schweppe likelihood ratio fully incorporates a Kalman filter, but also utilizes many more computations in evaluating the requisite Chernoff-like bounds needed in ROC tradeoff considerations in setting the operating point. All these aspects are simply illustrated here with a simple 2-state example so that qualitative insight can be gleaned from this in ascertaining how various parameters interact and influence the final tradeoff decision associated with operating point selection and fixed decision threshold specification/evaluation. This example is offered here because comparable examples for Schweppe's likelihood implementation appear to be lacking in the literature for anything other than the scalar single channel case. This two channel example is almost completely of closed form, but recourse is made to some simple FORTRAN computer programs for evaluating the two associated Chernoff-like bounds needed in the fundamental parametric study of allotted decision time interval versus associated false alarm and correct detection probabilities to be incurred.

II. 2-STATE SIGNAL MODEL FOR AN EXAMPLE SCHWEPPE'S LIKELIHOOD DETECTOR

The objective here is to evaluate the probabilities of correct detection and false alarm and to use these evaluations to select an appropriate decision threshold for a Schweppe likelihood-ratio implementation of a Neyman-Pearson receiver. This objective is to be carried out for a continuous-time second-order linear system having the structure depicted in Fig. 1 as representing the received signal content, corrupted by additive independent zero-mean Gaussian white noises in each of two measurement channels. The corresponding state variable representation of the system of Fig. 1 is as follows (consistent with the requirements of [14, sect. 2.1.5]):

$$\frac{d}{dt}\begin{bmatrix} x_1 \\ x_2 \end{bmatrix} = \begin{bmatrix} 0 & 1 \\ 0 & 0 \end{bmatrix}\begin{bmatrix} x_1 \\ x_2 \end{bmatrix} + \begin{bmatrix} 0 \\ 1 \end{bmatrix} u_1 \tag{1}$$

with statistics or associated expectations being

$$E[\mathbf{x}(0)] = \begin{bmatrix} \psi \\ \eta \end{bmatrix}; \qquad P_0 = \operatorname{cov}[\mathbf{x}(0)] = \begin{bmatrix} 2 & 0 \\ 0 & 2 \end{bmatrix};$$

$$E[u_1(t)u_1(\tau)] = \delta(t-\tau).$$

The measurement structure or outputs of the measurement sensors are correspondingly defined as

$$\mathbf{z} = \begin{bmatrix} z_1 \\ z_2 \end{bmatrix} = \begin{bmatrix} 1 & 0 \\ 0 & 2 \end{bmatrix}\begin{bmatrix} x_1 \\ x_2 \end{bmatrix} + \begin{bmatrix} 1 & 0 \\ 0 & 1 \end{bmatrix}\begin{bmatrix} v_1 \\ v_2 \end{bmatrix} \tag{2}$$

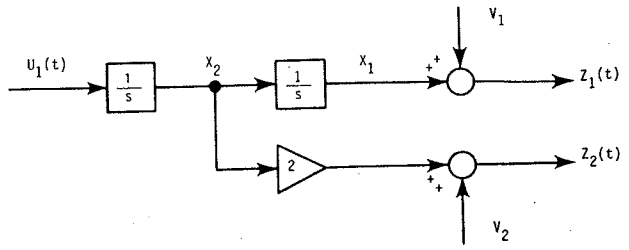

Fig. 1. Signal flow diagram depicting structure of particular signal to be detected.

with associated statistics

$$E[\mathbf{v}(t)\mathbf{v}^T(\tau)] = \begin{bmatrix} N & 0 \\ 0 & N \end{bmatrix}\delta(t-\tau),$$

where u_1, v_1, and v_2 are zero-mean independent, white Gaussian noises that are all uncorrelated with the Gaussian random vector initial condition $x(0)$, and $N \equiv \mathcal{N}_0/2$, where $\mathcal{N}_0/2$ is used in [14, p. 8] to represent the covariance intensity level of the white Gaussian measurement noise. In terms of fairly familiar standard notation for linear systems described by state variables, such as the convention utilized in [1], the following matrices suffice to summarize the parameter values to be encountered in the system depicted in Fig. 1:

$$F = \begin{bmatrix} 0 & 1 \\ 0 & 0 \end{bmatrix}; \qquad G = \begin{bmatrix} 0 \\ 1 \end{bmatrix};$$

$$H = \begin{bmatrix} 1 & 0 \\ 0 & 2 \end{bmatrix}; \qquad P_0 = \begin{bmatrix} 2 & 0 \\ 0 & 2 \end{bmatrix} \tag{3}$$

$$Q = I_{1\times 1}; \qquad R = \begin{bmatrix} N & 0 \\ 0 & N \end{bmatrix}; \qquad \bar{\mathbf{x}}(0) = \begin{bmatrix} \psi \\ \eta \end{bmatrix}. \tag{4}$$

Before proceeding too far, it is prudent first to test for *observability* of the system using the well-known Kalman rank test [1, p. 69] as

$$\operatorname{rank}[H^T \vdots F^T H^T] = \operatorname{rank}\begin{bmatrix} 1 & 0 & \vdots & 0 & 0 \\ 0 & 2 & \vdots & 1 & 0 \end{bmatrix} = 2 = n$$

since in the above

$$\det\begin{bmatrix} 1 & 0 \\ 0 & 2 \end{bmatrix} \neq 0$$

as a proper submatrix of the *observability Grammian*, the system is *observable*. Similarly, since

$$\operatorname{rank}[G \vdots FG] = \operatorname{rank}\begin{bmatrix} 0 & \vdots & 1 \\ 1 & \vdots & 0 \end{bmatrix} = 2 = n$$

and, consequently, the system is also *controllable* (i.e., randomness affects every state). If both *observability* and *controllability* conditions were not satisfied (or if *detectability* and *stability* conditions [2, pp. 82–83], which are somewhat weaker conditions more readily

satisfied by actual systems, were not satisfied) then it would be pointless to continue because a positive definite solution to the Riccati equation would no longer be guaranteed to exist, nor would the associated Kalman filter (to be utilized in mechanizing the likelihood ratio) be guaranteed to be exponentially asymptotically stable. However, for this example, observability and controllability *are* in fact satisfied as demonstrated above, so the solutions of the associated Riccati equation and Kalman filter are well behaved.

III. KALMAN FILTER-BASED VERSION OF SCHWEPPE LIKELIHOOD DETECTOR

The Kalman-Bucy filter that can be used to implement the Schweppe likelihood ratio [15, 16] solves the following two differential equations for the estimate and covariance, respectively:

$$\frac{d}{dt}\hat{\mathbf{x}}(t) = F\hat{\mathbf{x}}(t) + P(t)H^T R^{-1}[\mathbf{z}(t) - H\hat{\mathbf{x}}(t)] \quad (5)$$

with

$$\hat{\mathbf{x}}(0) = \begin{bmatrix}\psi \\ \eta\end{bmatrix}, \quad (6)$$

where $P(t)$ in the above is obtained as the solution of the Riccati equation:

$$\frac{d}{dt}P(t) = FP(t) + P(t)F^T - P(t)H^T R^{-1} HP(t) + GQG^T; \qquad P(0) = \begin{bmatrix}2 & 0 \\ 0 & 2\end{bmatrix}. \quad (7)$$

A unique solution to this covariance equation is guaranteed to exist and be positive definite since, as established above, (F,G) is a controllable pair, (H,F) is an observable pair, and *additionally* $P(0)$ above is obviously positive definite. For the parameters of this example, these two fundamental Kalman-Bucy filter equations become

$$\frac{d}{dt}\hat{\mathbf{x}}(t) = \begin{bmatrix}0 & 1 \\ 0 & 0\end{bmatrix}\hat{\mathbf{x}}(t) + P(t)\begin{bmatrix}1 & 0 \\ 0 & 2\end{bmatrix}\begin{bmatrix}1/N & 0 \\ 0 & 1/N\end{bmatrix} \times \left\{\mathbf{z}(t) - \begin{bmatrix}1 & 0 \\ 0 & 2\end{bmatrix}\hat{\mathbf{x}}(t)\right\} \quad (8)$$

with

$$\hat{\mathbf{x}}(0) = \begin{bmatrix}\psi \\ \eta\end{bmatrix} \quad (9)$$

and

$$\frac{d}{dt}P(t) = \begin{bmatrix}0 & 1 \\ 0 & 0\end{bmatrix}P(t) + P(t)\begin{bmatrix}0 & 0 \\ 1 & 0\end{bmatrix} - P(t)\begin{bmatrix}1 & 0 \\ 0 & 2\end{bmatrix}\begin{bmatrix}1/N & 0 \\ 0 & 1/N\end{bmatrix}\begin{bmatrix}1 & 0 \\ 0 & 2\end{bmatrix}P(t) + \begin{bmatrix}0 \\ 1\end{bmatrix}[1][0\ \ 1] \quad (10)$$

with

$$P(0) = \begin{bmatrix}2 & 0 \\ 0 & 2\end{bmatrix}. \quad (11)$$

Suppose that in the specific signal reception problem, interest is in whether the signal $x_2(t)$ is present in the received measurements or whether there is only noise v_2 present. Then the underlying hypothesis test is described by the following (cf., [14, eqs. (1), (2) on p. 8, eq. (88) on p. 26, eq. (112) on p. 31])

$$\mathcal{H}_1 : r(t) = [0\ \ 1]\begin{bmatrix}z_1 \\ z_2\end{bmatrix} = [0\ \ 1]\begin{bmatrix}1 & 0 \\ 0 & 2\end{bmatrix}\begin{bmatrix}x_1 \\ x_2\end{bmatrix} + [0\ \ 1]\begin{bmatrix}1 & 0 \\ 0 & 2\end{bmatrix}\begin{bmatrix}v_1 \\ v_2\end{bmatrix} = [0\ \ 2]\begin{bmatrix}x_1 \\ x_2\end{bmatrix} + v_2(t) \quad (12)$$

versus

$$\mathcal{H}_0 : r(t) = v_2(t), \quad (13)$$

where the effective observation matrix for this detection problem is, as seen from (12), to be $\tilde{H} = [0\ \ 2]$. The Riccati equation for the covariance of estimation error of the Kalman filter simplifies to

$$\frac{d}{dt}P(t) = \begin{bmatrix}0 & 1 \\ 0 & 0\end{bmatrix}P(t) + P(t)\begin{bmatrix}0 & 0 \\ 1 & 0\end{bmatrix} - P(t)\begin{bmatrix}0 \\ 2\end{bmatrix}\left[\frac{1}{N}\right][0\ \ 2]P(t) + \begin{bmatrix}0 & 0 \\ 0 & 1\end{bmatrix},$$

$$\text{with initial condition } P(0) = \begin{bmatrix}2 & 0 \\ 0 & 2\end{bmatrix}. \quad (14)$$

This is a nonlinear matrix Riccati equation of dimension $n = 2$, whose solution can be obtained by the standard device of solving a related linear problem of twice the dimension, $2n$, formed as

$$\frac{d}{dt}T(t) = \begin{bmatrix} F(t) & \vdots & G(t)QG^T(t) \\ \cdots & \cdots & \cdots \\ \tilde{H}^T(t)R^{-1}\tilde{H}(t) & \vdots & -F^T(t) \end{bmatrix} T(t) \quad (15)$$

with initial condition $T(0) = I_{2n\times 2n}$. In order to relate the solutions of (14) and (15), T is partitioned as

$$T(t) = \begin{bmatrix} T_{11} & \vdots & T_{12} \\ \cdots & \cdots & \cdots \\ T_{21} & \vdots & T_{22} \end{bmatrix} \quad (16)$$

from which a solution of the original covariance

equation can be obtained as

$$P(t) = (T_{11}P_0 + T_{12})(T_{21}P_0 + T_{22})^{-1} \triangleq \Gamma_1(t)\Gamma_2^{-1}(t). \tag{17}$$

For the parameters of the present example, the differential equation of (15) for the time evolution of the matrix $T(t)$ becomes

$$\frac{d}{dt}T(t) = \begin{bmatrix} 0 & 1 & \vdots & 0 & 0 \\ 0 & 0 & \vdots & 0 & 1 \\ \cdots & \cdots & \cdots & \cdots & \cdots \\ 0 & 0 & \vdots & 0 & 0 \\ 0 & \alpha^2 & \vdots & -1 & 0 \end{bmatrix} T(t) \tag{18}$$

It is easily demonstrated by hand calculations for the relatively sparse matrix B that

$$(sI - B)^{-1} = \frac{\text{adj}(sI - B)}{\det(sI - B)} = \begin{bmatrix} \frac{1}{s} & \frac{1}{s^2-\alpha^2} & \frac{-1}{s^2(s^2-\alpha^2)} & \frac{1}{s(s^2-\alpha^2)} \\ 0 & \frac{s}{s^2-\alpha^2} & \frac{-1}{s(s^2-\alpha^2)} & \frac{1}{s^2-\alpha^2} \\ 0 & 0 & \frac{1}{s} & 0 \\ 0 & \frac{\alpha^2}{s^2-\alpha^2} & \frac{-1}{s^2-\alpha^2} & \frac{s}{s^2-\alpha^2} \end{bmatrix}. \tag{20}$$

Using partial fraction expansions and appropriately inverse Laplace transforming (20) yields

$$T(t) = e^{Bt}T(0) = \mathcal{L}^{-1}\{(sI - B)^{-1}\} = \begin{bmatrix} 1 & \alpha^{-1}\sinh\alpha t & \vdots & \alpha^{-2}t - \alpha^{-3}\sinh\alpha t & -\alpha^{-2} + \alpha^{-2}\cosh\alpha t \\ 0 & \cosh\alpha t & \vdots & \alpha^{-2} - \alpha^{-2}\cosh\alpha t & \alpha^{-1}\sinh\alpha t \\ \cdots & \cdots & \cdots & \cdots & \cdots \\ 0 & 0 & \vdots & 1 & 0 \\ 0 & \alpha\sinh\alpha t & \vdots & -\alpha^{-1}\sinh\alpha t & \cosh\alpha t \end{bmatrix} \tag{21}$$

with $T(0) = I_{4\times4}$, where for convenience in notation we take

$$\alpha^2 \triangleq \frac{8}{\mathcal{N}_0} \equiv \frac{4}{N} \tag{19}$$

and where the matrix on the right hand side of the differential equation is denoted by B in what follows. The solution to (18) can be obtained by first finding $\mathcal{L}^{-1}\{(sI - B)^{-1}\}$, where s is the Laplace transform variable.

which also satisfies the initial condition $T(0) = I_{4\times4}$ as a check. Now according to (17) and [14, eq. (184) on p. 43]

$$\Gamma_1(t) = T_{11}P_0 + T_{12}; \qquad \Gamma_2(t) = T_{21}P_0 + T_{22} \tag{22}$$

and therefore,

$$\Gamma_1(t) = \begin{bmatrix} 2 + \alpha^{-2}t - \alpha^{-3}\sinh\alpha t & \vdots & 2\alpha^{-1}\sinh\alpha t + \alpha^{-2}\cosh\alpha t - \alpha^{-2} \\ \cdots & \cdots & \cdots \\ \alpha^{-2} - \alpha^{-2}\cosh\alpha t & \vdots & 2\cosh\alpha t + \alpha^{-1}\sinh\alpha t \end{bmatrix} \tag{23}$$

$$\Gamma_2(t) = \begin{bmatrix} 1 & \vdots & 0 \\ \cdots & \cdots & \cdots \\ -\alpha^{-1}\sinh\alpha t & \vdots & 2\alpha\sinh\alpha t + \cosh\alpha t \end{bmatrix} \tag{24}$$

from which we can reconstruct the final covariance of estimation error as

$$P(t) = \Gamma_1 \Gamma_2^{-1}. \tag{25}$$

Now, following [14, p. 24, eq. (77)], denote the desired signal as $\tilde{H}x$. Then the covariance of estimation error associated with this signal is [14, p. 24, eq. (85)]

$$\xi(t \mid \mathcal{S}(\cdot), N) \triangleq \tilde{H} P(t) \tilde{H}^T \tag{26}$$

where the notation $\xi(t \mid \mathcal{S}(\cdot), N)$, indicates that this is the covariance of the error in estimating the signal $x_2(t)$, where the intensity coefficient of the white noise that is corrupting the measurement is known to be N, and $\mathcal{S}(\cdot) \equiv x_2(\cdot)$ denotes the signal that is sought.

IV. QUALITATIVE ASPECTS OF DETECTOR PERFORMANCE

An intermediate parameter that is valuable in obtaining the probabilities of false alarm and correct detection, P_F and P_D, respectively, of the optimum Neyman-Pearson receiver (to be implemented as a Schweppe log-likelihood ratio [15]) is $\mu(s)$. Now in general:

$$\mu(s) = \mu_R(s) + \mu_D(s) \tag{27}$$

where $\mu_D(s) \equiv 0$ when the signal has a zero expected value. Here s is only an auxiliary parameter rather than being the Laplace variable encountered in (20). These two components of $\mu(s)$ are

$$\mu_R(s) \triangleq \frac{1}{2} \sum_{i=1}^{\infty} \left[(1-s) \ln\left(1 + \frac{\lambda_i}{N}\right) - \ln\left(1 + \frac{(1-s)\lambda_i}{N}\right) \right] \tag{28}$$

and

$$\mu_D(s) \triangleq -\frac{s}{2} \sum_{i=1}^{\infty} \frac{m_i^2}{\left|\frac{N}{(1-s)}\right| + \lambda_i} \tag{29}$$

where the λ_i in the above are obtained as solutions of the following integral equation:

$$\lambda_i \phi_i(t) = \int_{T_i}^{T_f} \tilde{H} E\left[\mathbf{x}(t)\mathbf{x}^T(u)\right] \tilde{H}^T \phi_i(u)\, du, \quad \text{for} \quad T_i \le t \le T_f \tag{30}$$

where T_i and T_f are the initial time and final completion times of signal reception. That is, the λ_i are the eigenvalues and the $\phi_i(t)$ are the orthonormal eigenfunctions[1] corresponding to the positive definite matrix

$$\tilde{H} E\left[\mathbf{x}(t)\mathbf{x}^T(u)\right] \tilde{H}^T \tag{31}$$

[1]Equations (28)–(30) pertain to an underlying Karhunen-Loeve series representation corresponding to the correlation function kernel of known structure.

with

$$\mathbf{m}_i \triangleq \int_{T_i}^{T_f} \left[\tilde{H} \Phi_F(t,0) \bar{\mathbf{x}}(0)\right] \phi_i(t)\, dt \tag{32}$$

where $\Phi_F(\cdot,\cdot)$ is the transition matrix associated with the system matrix F in (3). As spelled out in [14, p. 22, p. 36] and [17] for the appropriate evaluation procedure, certain useful identities can be introduced (as developed by Collins [18]) that relate the above infinite series to the integral of the covariance of the estimation error $\xi_P(t)$, which is already available as an adjunct to Kalman filter implementation and can be precomputed off-line. By exploiting these useful identities, no calculations are actually required from the unwieldy defining expressions of (28) and (29). In this vein, please consider the following representation [14, p. 47, eq. (215)]:

$$\mu_R(s) = \frac{(1-s)}{2N} \int_{T_i}^{T_f} \left[\xi_P(t \mid \mathcal{S}(\cdot), N) - \xi_P\left(t \mid \mathcal{S}(\cdot), \frac{N}{(1-s)}\right) \right] dt. \tag{33}$$

Even calculation with the less complicated expression of (33) can be entirely avoided by making use of yet another integral equality [17], [14, p. 44, eq. (195)] (and credited in [14, p. 44] to A. Baggeroer [24]):

$$\frac{1}{N} \int_{T_i}^{T_f} \xi_P(t \mid \mathcal{S}(\cdot), N)\, dt = \ln\left(\det\left[\Gamma_2(T_f)\right]\right) + \int_{T_i}^{T_f} \mathrm{tr}[F(t)]\, dt. \tag{34}$$

By exploiting the identity of (34) within (33), we find

$$\mu_R(s) = \frac{1}{2}(1-s)\left\{ \ln(\det[\Gamma_2(T_f)]) + \int_{T_i}^{T_f} \mathrm{tr}[F(t)]\, dt \right\} - \frac{1}{2}\left\{ \ln(\det[\Gamma_2(T_f)]) \,|_{\{\text{replace } \alpha \text{ throughout with } \alpha\sqrt{1-s}\}} + \int_{T_i}^{T_f} \mathrm{tr}[F(t)]\, dt \right\} \tag{35}$$

which for the parameter values of this example (as summarized in (3) and (4)) simplifies to

$$\mu_R(s) = \frac{(1-s)}{2} \ln[2\alpha \sinh(\alpha T_f) + \cosh(\alpha T_f)] - \frac{1}{2} \ln\left[2\alpha\sqrt{1-s} \sinh\left(\alpha\sqrt{1-s}\, T_f\right) + \cosh\left(\alpha\sqrt{1-s}\, T_f\right) \right]. \tag{36}$$

$$\ddot{\mu}_R(s) = \frac{\frac{(2+T_f)}{(1-s)}\tanh^2\left(\sqrt{1-s}T_f\right) + \frac{(2+T_f)}{2\left(\sqrt{1-s}\right)^3} + \frac{2T_f}{\sqrt{1-s}}\tanh\left(\sqrt{1-s}T_f\right)}{4\left[2\sqrt{1-s}\tanh\left(\sqrt{1-s}T_f\right)+1\right]^2}$$
$$+ \frac{\left[2T_f^2 - \frac{T_f(2+T_f)}{2(1-s)}\right]\operatorname{sech}^2\left(\sqrt{1-s}T_f\right)}{4\left[2\sqrt{1-s}\tanh\left(\sqrt{1-s}T_f\right)+1\right]^2}. \quad (40)$$

The term involving the integral in (35) has dropped out since the trace of F for this example is zero. The derivative of the expression of (36), with respect to the auxiliary parameter s, needed for eventual probability evaluation via a Chernoff-like bound, as in [14, sect. 2.2.2], is

$$\dot{\mu}_R(s) = -\frac{1}{2}\ln[2\alpha\sinh(\alpha T_f) + \cosh(\alpha T_f)]$$
$$+ \frac{1}{2}\frac{\frac{\alpha}{\sqrt{1-s}}\left(1+\frac{T_f}{2}\right)\sinh\left(\alpha\sqrt{1-s}T_f\right)}{\left[2\alpha\sqrt{1-s}\sinh\left(\alpha\sqrt{1-s}T_f\right)+\cosh\left(\alpha\sqrt{1-s}T_f\right)\right]}$$
$$+ \frac{1}{2}\frac{\alpha^2 T_f\cosh\left(\alpha\sqrt{1-s}T_f\right)}{\left[2\alpha\sqrt{1-s}\sinh\left(\alpha\sqrt{1-s}T_f\right)+\cosh\left(\alpha\sqrt{1-s}T_f\right)\right]}. \quad (37)$$

For concreteness in the present example and to allow a complete numerical evaluation, let the initial time be $T_i = 0$ s (sec) and the measurement noise intensity level be $\mathcal{N}_0 = 8$ squared units/s with the final time T_f remaining open for specification, but with a desired target false alarm of less than 0.1. Then the necessary expressions for $\mu_R(s)$, $\dot{\mu}_R(s)$, and $\ddot{\mu}_R(s)$ are found via differentiation with respect to s as, respectively,

$$\mu_R(s) = \frac{(1-s)}{2}\ln[2\sinh(T_f) + \cosh(T_f)]$$
$$- \frac{1}{2}\ln\left[2\sqrt{1-s}\sinh\left(\sqrt{1-s}T_f\right) + \cosh\left(\sqrt{1-s}T_f\right)\right] \quad (38)$$

and

$$\dot{\mu}_R(s) = -\frac{1}{2}\ln[2\sinh(T_f) + \cosh(T_f)]$$
$$+ \frac{1}{4}\frac{\frac{(2+T_f)}{\sqrt{1-s}}\tanh\left(\sqrt{1-s}T_f\right) + 2T_f}{\left[2\sqrt{1-s}\tanh\left(\sqrt{1-s}T_f\right)+1\right]} \quad (39)$$

and

The motivation for the reformulation of (39) in terms of $\tanh(\cdot)$ in place of the form of (37) is to simplify the implementation of the computer program to be used for explicit numerical evaluation, as presented in Section V.

Recapitulating for this example, the solution of the associated underlying state equation

$$\dot{\mathbf{x}}(t) = F(t)\mathbf{x}(t) + G(t)\mathbf{u}(t) \quad (41)$$

has the following form:

$$\mathbf{x}(t) = \Phi_F(t,0)\mathbf{x}(0) + \int_0^t \Phi_F(t,w)G(w)\mathbf{u}(w)\,dw. \quad (42)$$

Taking the expection throughout (42) yields a system mean of

$$\mathbf{m}_x(t) \triangleq E[\mathbf{x}(t)] = \Phi_F(t,0)E[\mathbf{x}(0)]$$
$$+ E\left[\int_0^t \Phi_F(t,w)G(w)\mathbf{u}(w)\,dw\right] \quad (43)$$

which simplifies to

$$\mathbf{m}_x(t) = \Phi_F(t,0)\bar{\mathbf{x}}(0) = \Phi_F(t,0)\begin{bmatrix}\psi\\ \eta\end{bmatrix} \quad \text{for time } t>0 \quad (44)$$

since the contribution of the second term on the right side of (43) is zero because the white noise has zero mean. Now

$$\mathcal{S}(t) = x_2(t) = \tilde{H}(t)\mathbf{x}(t) \quad (45)$$

so that

$$m_s(t) = E[\mathcal{S}(t)] = \tilde{H}(t)E[x(t)] = \tilde{H}(t)\Phi_F(t,0)\begin{bmatrix}\psi\\ \eta\end{bmatrix}. \quad (46)$$

For the parameters of this example, (46) is evaluated to be

$$m_s(t) = [0\ \ 2]\begin{bmatrix}1 & t\\ 0 & 1\end{bmatrix}\begin{bmatrix}\psi\\ \eta\end{bmatrix}$$
$$= [0\ \ 2]\begin{bmatrix}\psi\\ \eta\end{bmatrix} = 2\eta. \quad (47)$$

```
CALCROC     11:04EST

100* PROGRAM FINDS RECIEVER CHARACTERISTICS FOR THE TWO DIMENSIONAL EXAMPLE
101 DO 31 ITF=3,12,3
102 TF=ITF
110 PRINT 27
120 27 FORMAT(" RECIEVER OPERATING CHARACTERISTICS")
121 PRINT 26
122 26 FORMAT(" TF=")
123 PRINT 25,TF
124 25 FORMAT(1H,F5.1)
130 PRINT 28
140 28 FORMAT(" S        EMU        EMUD       EMUDD        PF         PM         PD")
150 ESINHT=(EXP(TF)-EXP(-1*TF))/2.
160 ECOSHT=(EXP(TF)+EXP(-1*TF))/2.
170 AUG1=2.*ESINHT+ECOSHT
180 PART1=(ALOG(AUG1))/2.
190 DO 30 I=1,19
200 SI=I
210 S=SI/20.
220 A1=1.-S
230 A2=SQRT(A1)
240 A4=TF*A2
250 HSIN=(EXP(A4)-EXP(-1.*A4))/2.
260 HCOS=(EXP(A4)+EXP(-1.*A4))/2.
270 HTAN=HSIN/HCOS
280 AUG2=2.*A2*HSIN+HCOS
290 PART2=.5*ALOG(AUG2)
300 EMU=A1*PART1-PART2
301 NUM1=((2.+TF)*HTAN)/A2+2.*TF
310 DENM1=2.*A2*HTAN+1.
320 EMUD=-PART1+NUM1/(4.*DENM1)
330 HSEC=(1./HCOS)
340 C1=(2.*(2.+TF))/A1
350 C2=(2.+TF)/(2.*A1*A2)+(2.*TF)/A2
360 C3=2.*TF*TF-((2.+TF)*TF)/(2.*A1)
370 HSEC2=HSEC*HSEC
380 HTAN2=HTAN*HTAN
390 NUM2=C1*HTAN2+C2*HTAN+C3*HSEC2
400 DENM2=DENM1*DENM1
410 EMUDD=(0.25*NUM2)/DENM2
420 SF1=1./SQRT(6.283*S*S*EMUDD)
430 SF2=1./SQRT(6.283*A1*A1*EMUDD)
440 FBEX=EMU-S*EMUD
450 EMBEX=EMU+A1*EMUD
460 FB=EXP(FIEX)
470 EMB=EXP(EMBEX)
480 PF=SF1*FB
490 PM=SF2*EMB
500 PD=1.-PM
510 PRINT 29,S,EMU,EMUD,EMUDD,PF,PM,PD
520 29 FORMAT(1H,F4.2,F10.4,F10.4,F10.4,4X,F6.3,4X,F6.3,4X,F6.3)
530 30 CONTINUE
531 31 CONTINUE
540 STOP;END
```

Fig. 2. FORTRAN computer program used to evaluate P_F and P_D for the particular detection example.

If $\eta \neq 0$ in the above, then the signal anticipated for reception does *not* have a zero-mean function.

The component $\mu_D(s,t)$, required when the signal is not of zero mean, can be calculated as the output of the dynamic system depicted in Fig. 9 (see the Appendix). However, to simplify this example, it is assumed here that in fact $\eta \equiv 0$. Then (47) simplifies to $m_s(t) = 0$, and (29) simplifies to $\mu_D(s) = 0$. Therefore, for this example, the general expression of (27) degenerates to

$$\mu(s) = \mu_R(s). \tag{48}$$

V. EVALUATION OF PERFORMANCE TRADEOFFS USING CHERNOFF-LIKE BOUNDS

Motivated by the Chernoff bound (as derived by [19, pp. 121–122] and demonstrated to be appropriate and optimized to be tight by [14, pp. 38–41] for problems of the form of this example), the approximate expression for P_F, the probability of a false alarm within the time interval, is

$$P_F \simeq \frac{1}{\sqrt{2\pi s^2 \ddot{\mu}(s)}} \exp[\mu(s) - s\dot{\mu}(s)], \qquad \text{for} \quad 0 \leq s \leq 1 \tag{49}$$

and, correspondingly, the approximate expression for P_M, the probability of a miss within the time interval, is

$$P_M = 1 - P_D \simeq \frac{1}{\sqrt{2\pi(1-s)^2 \ddot{\mu}(s)}} \times \exp[\mu(s) + (1-s)\dot{\mu}(s)], \qquad \text{for} \quad 0 \leq s \leq 1 \tag{50}$$

with P_D, being the probability of correct detection.

These probabilities are evaluated here for a range of values of the auxiliary parameter s. The tabulated results are depicted in Figs. 3 and 4 for the parameters of this example using the simple FORTRAN computer program depicted in Fig. 2. The dependence on s

```
CALCROC

RECIEVER OPERATING CHARACTERISTICS
TF=
  3.0
s        EMU        EMUD       EMUDD        PF         PM         PD
0.05   -0.0386   -0.7664    0.5502    10.754     0.263      0.737
0.10   -0.0757   -0.7490    0.6009     5.142     0.270      0.730
0.15   -0.1114   -0.7304    0.6558     3.278     0.279      0.721
0.20   -0.1454   -0.7103    0.7157     2.350     0.289      0.711
0.25   -0.1775   -0.6887    0.7812     1.796     0.301      0.699
0.30   -0.2076   -0.6651    0.8891     1.399     0.308      0.692
0.35   -0.2355   -0.5427    1.0085     1.085     0.339      0.661
0.40   -0.2608   -0.5117    1.1419     0.882     0.353      0.647
0.45   -0.2832   -0.4773    1.2922     0.728     0.370      0.630
0.50   -0.3024   -0.4387    1.5080     0.598     0.386      0.614
0.55   -0.3177   -0.2859    1.7569     0.466     0.428      0.572
0.60   -0.3286   -0.2312    2.1000     0.379     0.452      0.548
0.65   -0.3342   -0.1672    2.5657     0.306     0.480      0.520
0.70   -0.3333    0.0334    3.1971     0.223     0.538      0.462
0.75   -0.3244    0.2660    4.0638     0.156     0.612      0.388
0.80   -0.3051    0.4044    5.4444     0.114     0.683      0.317
0.85   -0.2720    0.7420    7.6550     0.069     0.819      0.181
0.90   -0.2192    1.1938   11.7248     0.036     1.054     -0.054
0.95   -0.1361    2.0620   20.0971     0.012     1.722     -0.722
RECIEVER OPERATING CHARACTERISTICS
TF=
  6.0
s        EMU        EMUD       EMUDD        PF         PM         PD
0.05   -0.0757   -1.5074    0.9484     8.191     0.095      0.905
0.10   -0.1489   -1.4770    1.0424     3.903     0.099      0.901
0.15   -0.2196   -1.4446    1.1128     2.514     0.105      0.895
0.20   -0.2873   -1.4098    1.2537     1.772     0.108      0.892
0.25   -0.3520   -1.2810    1.3733     1.319     0.122      0.878
0.30   -0.4131   -1.2388    1.5394     1.028     0.128      0.872
0.35   -0.4705   -1.1930    1.7219     0.824     0.135      0.865
0.40   -0.5235   -1.0449    1.9240     0.647     0.152      0.848
0.45   -0.5716   -0.9875    2.2305     0.523     0.159      0.841
0.50   -0.6141   -0.8204    2.5748     0.406     0.179      0.821
0.55   -0.6501   -0.7463    3.0113     0.329     0.191      0.809
0.60   -0.6784   -0.5521    3.6104     0.247     0.214      0.786
0.65   -0.6977   -0.3374    4.4662     0.180     0.239      0.761
0.70   -0.7056   -0.0962    5.6582     0.127     0.268      0.732
0.75   -0.6993    0.1806    7.4116     0.085     0.305      0.695
0.80   -0.6741    0.6412   10.4008     0.047     0.358      0.642
0.85   -0.6223    1.3430   15.9014     0.020     0.438      0.562
0.90   -0.5294    2.4060   27.9628     0.006     0.565      0.435
0.95   -0.3618    4.5311   65.2140     0.000     0.863      0.137

While exact probabilities must lie between zero and one, the approximate expressions of Eqs. 49 and 50
are neither tight nor accurate near the extremes of s=0 or s=1. The result of eliminating s in the above
evaluations : probabilities versus s yields only probabilities of interest that are between zero and one
for P_f vs P_D.
```

Fig. 3. P_F and P_D versus the auxiliary parameter s as output from the computer program (for final times of $T_f = 3$ and 6 seconds).

was further mutually eliminated to obtain plots of P_D versus P_F (depicted in Fig. 5 and uniquely summarized in the 3-dimensional view in Fig. 6 as the knee of the ROC curve becomes more pronounced as a function of an increasing detection interval) to provide insight into how the choice of T_f radically affects the ROCs for the Schweppe likelihood ratio detector of this example.

From the family of ROCs considered, it is decided to use $T_f = 9$ s as a satisfactory decision interval since the achievable detection probabilities are sufficiently high (i.e., P_f less than 0.1 and with a P_D greater than 0.8, as sought and specified above). The ROC for this *now* fixed decision interval is summarized in Fig. 7.

The slope of the tangent to the ROC at the operating point that is decided upon (here $P_F = 0.075$, $P_D = 0.845$) is 18/28. This is the threshold value that the likelihood ratio will be compared against (as $\gamma = 18/28$) in making a decision on whether the desired signal was in fact received or whether only noise was received.

In summary, the dynamic system depicted in Fig. 8 illustrates how the optimum Schweppe likelihood ratio detector can be implemented using only simple squaring and averaging operations on the output of a Kalman filter. This example has been offered to illustrate what steps must be followed in order to evaluate P_D and P_F using the approximate Chernoff-bound method. As mentioned at the bottom of Figs. 3 and 4, inaccuracies in Chernoff bound approximation occur at the extremes of $s = 0$ and $s = 1$. However, when the parametric dependence on s is eliminated between P_D and P_F, as depicted in the four plots of Fig. 5, there are no upsetting nonintuitive anomalies observed in this same data within the region of interest from $(P_D, P_F) = (0,0)$ to $(1,1)$ when viewed from this perspective. The author has demonstrated different P_D and P_F evaluation techniques for other algorithms in [20–22]. The generally lower detection probabilities exibited in this example correspond to expected levels of certain error signals typical of navigation systems in seeking to detect soft failures, as

TF=
9:0

S	EMU	EMUD	EMUDD	PF	PM	PD
0.05	-0.1127	-2.2446	1.3508	6.862	0.038	0.962
0.10	-0.2219	-2.2005	1.4592	3.296	0.041	0.959
0.15	-0.3275	-2.1534	1.6074	2.088	0.043	0.957
0.20	-0.4290	-2.0135	1.7679	1.461	0.049	0.951
0.25	-0.5260	-1.9575	1.9426	1.104	0.052	0.948
0.30	-0.6181	-1.8037	2.1689	0.836	0.059	0.941
0.35	-0.7048	-1.7362	2.4176	0.665	0.063	0.937
0.40	-0.7854	-1.5645	2.7315	0.514	0.072	0.928
0.45	-0.8590	-1.4811	3.1217	0.414	0.077	0.923
0.50	-0.9247	-1.2855	3.6459	0.315	0.087	0.913
0.55	-0.9813	-1.0728	4.2402	0.238	0.100	0.900
0.60	-1.0272	-0.8394	5.1173	0.174	0.113	0.887
0.65	-1.0601	-0.5803	6.2419	0.124	0.129	0.871
0.70	-1.0772	-0.1688	7.9150	0.078	0.153	0.847
0.75	-1.0743	0.1729	10.4401	0.049	0.176	0.824
0.80	-1.0448	0.8415	14.7071	0.023	0.217	0.783
0.85	-0.9777	1.7829	22.7414	0.008	0.274	0.726
0.90	-0.8516	3.2815	41.5873	0.002	0.367	0.633
0.95	-0.6127	6.6489	110.2850	0.000	0.574	0.426

RECIEVER OPERATING CHARACTERISTICS

TF=
12.0

S	EMU	EMUD	EMUDD	PF	PM	PD
0.05	-0.1497	-2.9817	1.7531	6.022	0.016	0.984
0.10	-0.2950	-2.9239	1.9060	2.882	0.017	0.983
0.15	-0.4354	-2.7744	2.0710	1.813	0.020	0.990
0.20	-0.5706	-2.7067	2.2822	1.282	0.021	0.979
0.25	-0.7001	-2.5425	2.5120	0.944	0.025	0.975
0.30	-0.8231	-2.4621	2.7985	0.731	0.027	0.973
0.35	-0.9391	-2.2792	3.1502	0.558	0.031	0.969
0.40	-1.0473	-2.0838	3.5393	0.428	0.036	0.964
0.45	-1.1464	-1.9744	4.0542	0.340	0.039	0.961
0.50	-1.2354	-1.7499	4.6754	0.257	0.045	0.955
0.55	-1.3125	-1.5052	5.5168	0.190	0.052	0.948
0.60	-1.3758	-1.1253	6.5792	0.129	0.063	0.937
0.65	-1.4225	-0.8208	8.0773	0.089	0.073	0.927
0.70	-1.4488	-0.3567	10.1916	0.054	0.088	0.912
0.75	-1.4493	0.1723	13.4377	0.030	0.107	0.893
0.80	-1.4156	1.0555	18.8787	0.012	0.138	0.862
0.85	-1.3336	2.2506	29.2185	0.003	0.182	0.818
0.90	-1.1756	4.2151	53.9840	0.000	0.255	0.745
0.95	-0.8706	8.6962	150.0665	0.000	0.421	0.579

While exact probabilities must lie between zero and one, the approximate expressions of Eqs. 49 and 50 are neither tight nor accurate near the extremes of s=0 or s=1. The result of eliminating s in the above evaluations of probabilities versus s yields only probabilities of interest that are between zero and one for P_F vs. P_D.

Fig. 4. P_F and P_D versus the auxiliary parameter s as output from the computer program (for final times of $T_f = 9$ and 12 seconds).

discussed in [27], when posed as a Schweppe likelihood detection problem instead of as posed in [20, 21, or 27]. This concludes this example by completely discussing all its aspects.

Historical perspective is provided in [17] on how the results of [15], as used here, were a fundamental breakthrough in circumventing the previous barrier consisting of the difficult task of having to solve an intractable Fredholm integral equation in order to specify the impulse response of the optimal receiver structure by, instead, merely mathematically massaging the outputs of an associated Kalman filter as just squaring and averaging operations to more simply realize the optimal receiver. Although the simple closed-form example presented here is completely stationary by having only constant matrix parameters in (5), the techniques of [15] can handle detection of certain nonstationary signal structures as well (corresponding to having specified time-varying matrices within (3), (4), (41)) within the stationary white measurement noise by using this Kalman filter-based approach.

Recent generaiizations in the three directions of mathematical derivation, physical interpretation, and hardware implementation of optimal receiver structures are provided in [26] in terms of newly developed time-frequency plane techniques. The approach of [26] allows a narrowing of attention to concentrated regions of interest in the time-frequency plane through recourse to an underlying cross-Wigner-Ville distribution, use of an ancillary condition that the two-dimensional Fourier transform of an associated weighting function be of constant modulus, and use of ambiguity function manipulations previously familiar from radar and sonar applications.

APPENDIX A. DYNAMICAL SYSTEM FOR GENERATING $\mu_D(S)$, IF SIGNAL HAS NONZERO MEAN

Consider the problem of evaluating $\mu_D(s)$ of (29) ([14, problem 2.2.1 on p. 53]), which is equivalently given by [14, eq. (135) on p. 36]

$$\mu_D(s) = -\frac{s}{2}\int_0^T m(t)g(t \mid \beta(s))\,dt. \qquad (51)$$

where $\beta(s) = 2(1-s)/\mathcal{N}_0$.

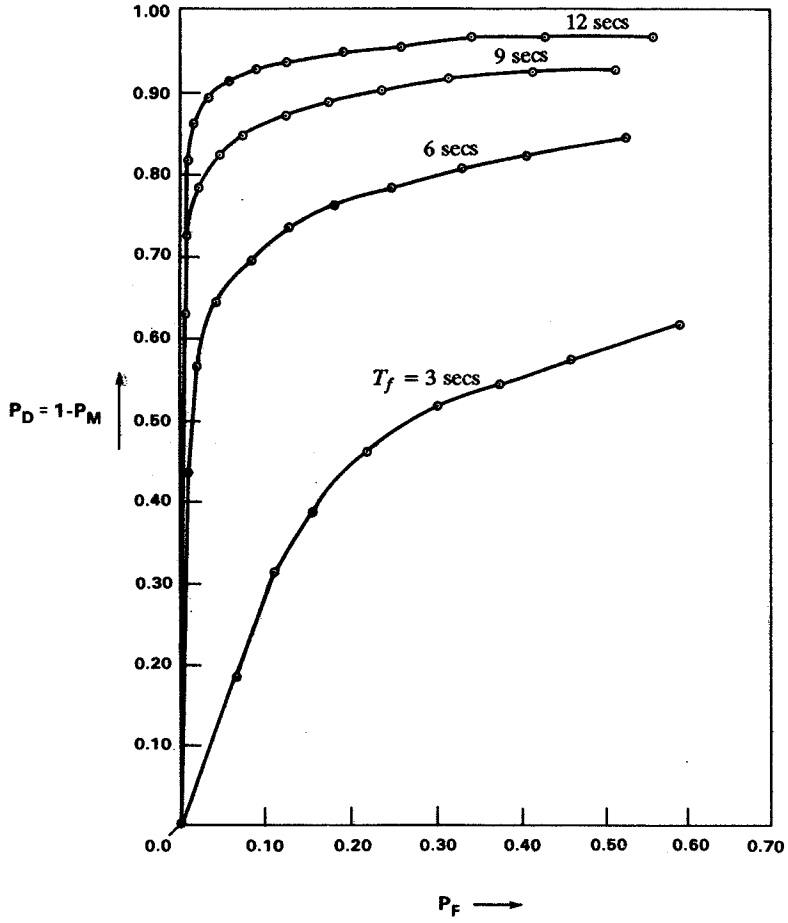

Fig. 5. Optimum ROC for $T_f = 3, 6, 9, 12$ s.

Assuming that $S(t)$ has a finite dimensional state space representation, as utilized in (1), (41), and (45), further define $\mu_D(\cdot)$ more explicitly as a function of two variables:

$$\mu_D(s,T) = -\frac{s}{2}\int_0^T m(w)g(w \mid \beta(s))\,dw. \qquad (52)$$

The objective here is to find a finite dimensional dynamic system whose output is $\mu_D(s,T)$, as associated with detecting a signal of nonzero mean.

Solution:

From (52),

$$\mu_D(s,t) = -\frac{s}{2}\int_0^t m(w)g(w \mid \beta(s))\,dw \quad \text{for} \quad 0 \le t \le T. \qquad (53)$$

By Leibnitz's rule for differentiating an integral, we have that

$$\frac{d}{dt}\mu_D(s,t) = -\frac{s}{2}m(t)g(t \mid \beta(s)) \quad \text{for} \quad 0 \le t \le T \qquad (54)$$

with

$$g(u \mid \beta(s)) \triangleq \int_0^T m(w)Q_1(w,u;s)\,dw, \quad \text{for} \quad 0 \le t \le T \qquad (55)$$

$$Q_1(w,u;s) = \beta(s)\{\delta(w-u) - h_1(w,u;s)\}, \quad \text{for} \quad 0 \le w,u \le T \qquad (56)$$

where $h_1(t,u;s)$ denotes the impulse response of an associated Kalman-Bucy filter, specified by the solution to the following differential equations:

$$\frac{d}{dt}\hat{x}(t;s) = [F(t) - \xi_p(t;s)H^T(t)\{\beta(s)\}H(t)]\hat{x}(t;s) + \xi_p(t;s)H^T(t)\{\beta(s)\}r(t) \qquad (57)$$

$$\frac{d}{dt}\xi_p(t;s) = F(t)\xi_p(t;s) + \xi_p(t;s)F^T(t) - \xi_p(t;s)H^T\{\beta(s)\}H(t)\xi_p(t;s) + GQG^T \qquad (58)$$

with initial condition

$$\xi_p(0;s) = E[(\mathbf{x}(0) - \bar{\mathbf{x}}(0))(\mathbf{x}(0) - \bar{\mathbf{x}}(0))^T]. \qquad (59)$$

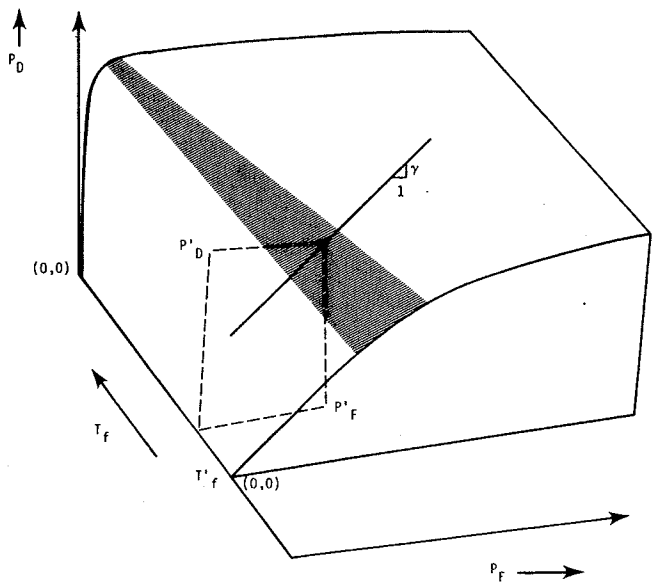

Fig. 6. ROCs as functions of T_f (decision interval).

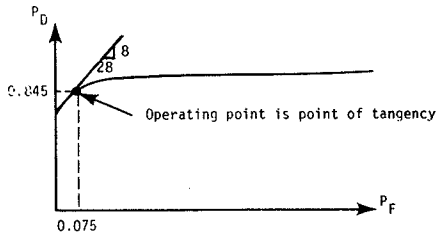

Fig. 7. Decision threshold used is slope of tangent ROC curve at operating point. P_D and P_F are fixed by this operating point.

Now, the expression for $g(u \mid \beta(s))$ in (55) can be evaluated by substituting for $Q_1(w,u;s)$ from (56) to yield

$$g(u \mid \beta(s)) = \int_0^t m(w)\beta(s)\{\delta(w-u) - h_1(w,u;s)\}\,dw$$
$$= \beta(s)\left\{m(u) - \int_0^t m(w)h_1(w,u;s)\,dw\right\}. \tag{60}$$

Equations (57), (58), (60), and (54) for $0 \le t \le T$, and $0 \le s < 1$, completely specify a dynamic system which can generate $\mu_D(s,t)$, which at time $t = T$ is $\mu_D(s,T)$. From (57), the requisite Kalman filter impulse response is observed to be

$$h_1(w,u;s) = H(w)\Phi_K(w,u;s)\xi_p(u;s)H^T(u)[\beta(s)] \tag{61}$$

where $\Phi_K(w,u;s)$ satisfies the following well-known partial differential equation for the associated transition matrix

$$\frac{\partial}{\partial t}\Phi_K(t,u;s) = [F(t) - \xi_p(t;s)H^T(t)\{\beta(s)\}H(t)]$$
$$\times \Phi_K(t,u;s) \tag{62}$$

with

$$\Phi_K(t,t;s) = I \qquad \text{for all } t \tag{63}$$

and $\xi_p(t;s)$ in (61) and (62) is the solution of (58). A realization of this impulse response as a dynamic system for generating $\mu_D(s,t)$ is as depicted in the system block diagram of Fig. 9.

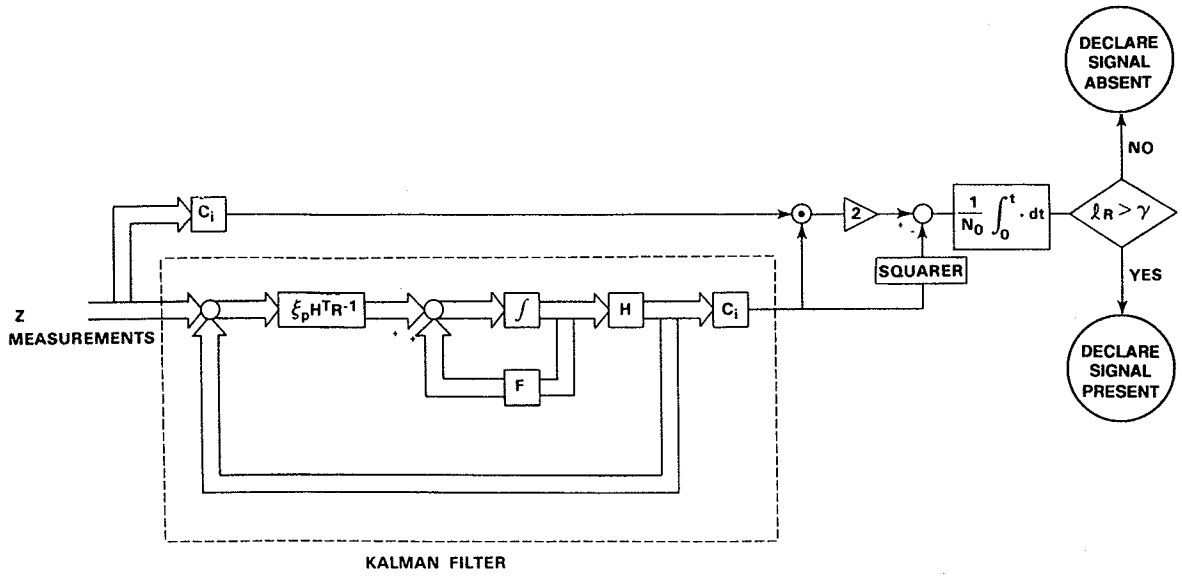

Fig. 8. Kalman filter-based implementation of Schweppe likelihood ratio for optimum detection of random signal of known statistics in additive zero-mean Gaussian white noise.

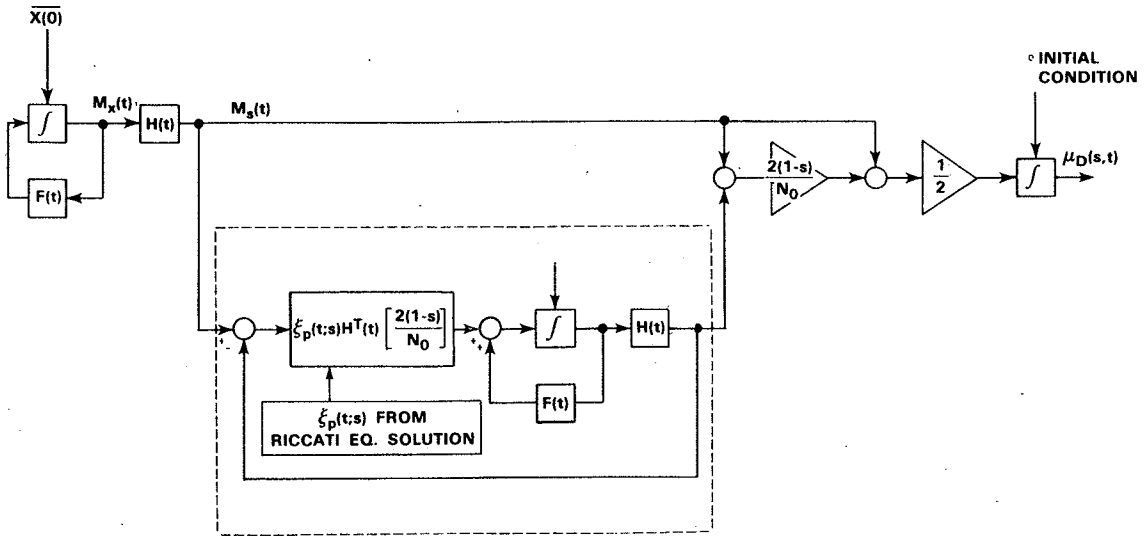

Fig. 9. Dynamic system for generating μ_D as needed for Schweppe likelihood detector in general case for detecting signal not of zero mean.

DEDICATION

This paper is offered as a tribute to the memory of a great man who died during the summer of 1988.

ACKNOWLEDGMENT

Thanks are due to an anonamous reviewer who suggested that the example closed-form answers provided here could also be used as a test gauge as another non-Chernoff-based approach is pursued for the evaluation of the probabilities of correct detection and false alarm for a Schweppe's likelihood detector as a possible improvement to the current state of the art evaluation methodology. This attempted refinement is currently underway.

REFERENCES

[1] Gelb, A. (Ed.) (1974)
Applied Optimal Estimation.
Cambridge, MA: MIT Press, 1974.

[2] Anderson, B. D. O., and Moore, J. B. (1979)
Optimal Filtering.
Englewood Cliffs, NJ: Prentice-Hall, 1979.

[3] Fitzgerald, R. J. (1981)
Simple tracking filters: closed-form solutions.
IEEE Transactions on Aerospace and Electronic Systems, **AES-17**, 6 (Nov. 1981), 781–785.

[4] Farrenkopf, R. L. (1978)
Analytic steady-state accuracy solutions for two common spacecraft attitude estimators.
AIAA Journal of Guidance and Control, **1** (July–Aug. 1978), 282–284.

[5] Castella, F. R. (1981)
Tracking accuracies with position and rate measurements.
IEEE Transactions on Aerospace and Electronic Systems, **AES-17**, 3 (May 1981), 433–437.

[6] Friedland, B. (1973)
Optimum steady-state position and velocity estimation using noisy sampled position data.
IEEE Transactions on Aerospace and Electronic Systems, **AES-9**, 6 (Nov. 1973), 906–911.

[7] Ramachandra, K. V. (1983)
Analytical results for a Kalman tracker using position and rate measurements.
IEEE Transactions on Aerospace and Electronic Systems, **AES-19**, 5 (Sept. 1983), 776–778.

[8] Ekstrand, B. (1983)
Analytical steady-state solution for a Kalman tracking filter.
IEEE Transactions on Aerospace and Electronic Systems, **AES-19**, 6 (Nov. 1983), 815–819.

[9] Gupta, S. N. (1985)
An extension of 'Closed-form solutions of target-tracking filters with discrete measurements.'
IEEE Transactions on Aerospace and Electronic Systems, **AES-20**, 6 (Nov. 1985), 839–841.

[10] Yu, M. H., and Meyer, M. P. (1985)
Closed-form solution of a recursive tracking filter with a priori velocity initialization.
IEEE Transactions on Aerospace and Electronic Systems, **AES-21**, 2 (Mar. 1985), 262–264.

[11] Ramachandra, K. V. (1987)
Identical steady-state results for a Kalman tracker.
IEEE Transactions on Aerospace and Electronic Systems, **AES-23**, 1 (Jan. 1987), 129–130; (corrections in **AES-23**, 2 (Mar. 1987), 294.

[12] Grimble, M. J., and Astrom, K. J. (1987)
Frequency domain properties of Kalman filters.
International Journal of Control, **45**, 3 (1987), 907–925.

[13] Meditch, J. S. (1969)
Stochastic Optimal Linear Estimation and Control.
New York: McGraw-Hill, 1969.

[14] Van Trees, H. L. (1971)
Detection, Estimation and Modulation Theory, Part III: Radar-Sonar Signal Processing and Gaussian Signals in Noise.
New York: Wiley, 1971.

[15] Schweppe, F. C. (1965)
Evaluation of likelihood functions for Gaussian signals.
IEEE Transactions on Information Theory, **IT-11** (Jan. 1965), 61–70.

[16] Rajasekaran, P. K., and Srinath, M. D. (1971)
Structure and parameter adaptive pattern recognition with supervised learning: a new formulation.
IEEE Transactions on Information Theory, **IT-17**, 4 (July 1971), 499–500.

[17] Van Trees, H. L. (1970)
Applications of state variable techniques in detection theory.
Proceedings of the IEEE, **58**, 5 (May 1970), 653–669.

[18] Collins, L. D. (1968)
Closed-form expressions for the Fredholm determinant for state variable covariance functions.
Proceedings of the IEEE, **56**, 3 (Mar. 1968), 350–351.

[19] Van Trees, H. L. (1968)
Detection, Estimation, and Modulation Theory, Part I: Detection, Estimation, and Linear Modulation Theory.
New York: Wiley, 1968.

[20] Kerr, T. H. (1980)
Statistical analysis of a two ellipsoid overlap test for real-time failure detection.
IEEE Transactions on Automatic Control, **AC-25**, 4 (Aug. 1980), 762–772.

[21] Kerr, T. H. (1982)
False alarm and correct detection probabilities over a time interval for restricted classes of failure detection algorithms.
IEEE Transactions on Information Theory, **IT-28**, 4 (July 1982), 619–631.

[22] Kerr, T. H. (1982)
Impact of navigation accuracy in optimized straight-line surveillance/detection of undersea buried pipe valves.
In *Proceedings of National Marine Meeting of the Institute of Navigation*, Cambridge, MA, Oct. 27–29, 1982, 70–80.

[23] Ramachandra, K. V. (1987)
Optimum steady state position, velocity, and acceleration estimation using noisy sampled position data.
IEEE Transactions on Aerospace and Electronic Systems, **AES-23**, 5 (Sept. 1987), 705–708 (corrections in **AES-24**, 3 (May 1988), 316).

[24] Baggeroer, A. (1969)
A state-variable approach to the solution of fredholm integral equations.
IEEE Transactions on Information Theory, **IT-15**, 5 (Sept. 1969), 557–570.

[25] Fitzgerald, R. J. (1980)
Simple tracking filters: steady-state filtering and smoothing performance.
IEEE Transactions on Aerospace and Electronic Systems, **AES-16**, 6 (Nov. 1980), 860–864 (with minor corrections in **AES-17**, 2 (Mar. 1981), 305).

[26] Flandrin, P. (1988)
A time-frequency formulation of optimum detection.
IEEE Transactions on Acoustics, Speech, and Signal Processing, **ASSP-36**, 9 (Sept. 1988), 1377–1384.

[27] Kerr, T. H. (1987)
Decentralized filtering and redundancy management for multisensor navigation.
IEEE Transactions on Aerospace and Electronic Systems, **AES-23**, 1 (Jan. 1987), 83–119 (minor corrections appear in **AES-23**, 3 (May 1987), 412 and **AES-23**, 4 (July 1987), 599).

Thomas Kerr (S'67—M'74—SM'85) was born in Washington, D.C. on November 9, 1945. He received the B.S.E.E. (magna cum laude) from Howard University, Washington, D.C. in 1967 and the M.S. and Ph.D. degrees (via NSF) in the electrical engineering specialty of control/estimation from the University of Iowa, Iowa City, IA, in 1969 and 1971, respectively.

A staff member at M.I.T. Lincoln Laboratory since October 1986 in the area of spectral estimation (which uses the same estimation/detection/identification/pattern recognition tools) and use of Extended Kalman filters for radar tracking applications, he had been a senior analyst/systems engineer at Intermetrics since 1979 with interests in navigation system and sonobuoy system tracking/implementation/Kalman filtering/failure detection. His previous experience includes university teaching/research (1967–1971), analysis, computer simulation, and real-time implementation at General Electric's Corporate R&D Center in Schenectady, NY (1971–1973), and navigation/filtering/failure detection applications at TASC (1973–1979).

His Department of Defense application involvements include: investigations and computer implementations of parameter identification, mathematical and algorithmic aspects of estimation and control, decentralized and nonlinear filtering, and quantifying associated computer burdens, hypothesis testing/failure detection, effects of failure detection on the reliability/availability of reconfigurable modular composite systems, bicriteria (Pareto-) optimization algorithms, and procedures for Kalman filter sensor selection and scheduling, tractable applications of level-crossing theory, point-process detection in antisubmarine warfare, optimal search and screening techniques, multitarget tracking, RV target tracking and angles-only triangulation tracking, and pattern recognition. These above investigations were performed for various applications including Poseidon and Trident SINS/ESGN navigation systems, JTIDS RelNav, ICNIA and other GPS-aided multisensor avionics navigation applications, minesweeper PINS, PTA sonobuoy tracking, post-coherence function sonobuoy target tracking, ASW search, submarine antenna detectability to radar surveillance, helicopter-based Missile Warning System development and refinement, SDI satellite survivability, and BSD countermeasures.

Dr. Kerr is also a member of Tau Beta Pi, Eta Kappa Nu, Sigma Pi Sigma, Pi Mu Epsilon, AIAA, ION, AAAS, the Naval Institute, ADPA, NSIA, and IEEE AC, IT, AES, and ASSP groups, and CRW.